

Cavity-assisted generation of entangled photon pairs by a quantum-dot cascade decay

F. Troiani

*Departamento de Física Teórica de la Materia Condensada, Universidad Autónoma de Madrid, Cantoblanco 28049 Madrid, Spain
and CNR-INFM National Research Center on nano-Structures and bio-Systems at Surfaces (S3), 41100 Modena, Italy*

J. I. Perea and C. Tejedor

Departamento de Física Teórica de la Materia Condensada, Universidad Autónoma de Madrid, Cantoblanco 28049 Madrid, Spain

(Received 15 September 2006; published 7 December 2006)

We compute the concurrence of the polarization-entangled photon pairs generated by the biexciton cascade decay of a semiconductor quantum dot. We show how a cavity-induced increase of the photon emission rate reduces the effect of dot dephasing and excitonic fine structure on the concurrence. However, strong dot-cavity couplings, as well as low detection efficiencies, increase the detrimental effect of multiple cascades. This affects the merits of the entangled photon-pair source, beyond what is estimated by quantum tomography.

DOI: [10.1103/PhysRevB.74.235310](https://doi.org/10.1103/PhysRevB.74.235310)

PACS number(s): 78.67.Hc, 03.67.Hk, 42.50.Dv

I. INTRODUCTION

Most protocols in optical quantum-information processing require deterministic sources of entangled photon pairs.¹ It has been argued that semiconductor quantum dots (QDs) might represent the active element of such a quantum device.^{2,3} In fact, first proofs of principle have been recently established, where entanglement between the polarization and frequency degrees of freedom has been measured in photon pairs generated by the cascade emission from single QDs.^{4,5} However, the degree of entanglement is still limited by the dot dephasing, the excitonic fine-structure splitting, and the mixed nature of the dot state, resulting from its incoherent (i.e., off-resonant) excitation. It is believed that these limitations can be to a large extent overcome by increasing the photon emission rate, through the embedding of the QD in a semiconductor microcavity (MC).⁶ The development of more sophisticated devices and excitation strategies is also being considered.^{7,8} In spite of such great interest, a clear theoretical interpretation of the recent experimental achievements is not currently available. It is the goal of the present paper to provide such an understanding, and the resulting indications for the future development of entangled-photon sources.

The paper is organized as follows. Section II describes how the density matrix of the emitted photon pairs can be derived from the dynamics of the dot-cavity system. In Sec. III, we first present how such dynamics depends on the relevant physical parameters and on the exciting conditions; then, we analyze the merits of the photon-pair source, by including the effects of the detection efficiency. Finally, a brief summary is given in Sec. IV.

II. MODEL

The origin of the polarization-frequency entanglement in the photon pair resides in the QD's low-energy level scheme [Fig. 1(a)]. This includes the biexciton level (B), the two lowest exciton ones (X_H and X_V), and the ground state (G). The radiative relaxation of the dot from B to G can take place along two paths, which result in the emission of light

with either horizontal (H) or vertical (V) linear polarization. The photons generated by the biexciton and exciton decays (1 and 2, respectively) differ in frequency due to the biexciton binding energy $\Delta = \omega_2 - \omega_1$. In the ideal case, the dot is initially driven to $|B\rangle$, and subsequently relaxes, generating the maximally entangled two-photon state

$$|\psi\rangle = (|H1, H2\rangle + e^{i\phi}|V1, V2\rangle)/\sqrt{2}$$

by cascade emission. In realistic exciting conditions, however, the state of the emitted radiation ρ_{ph} is affected by a number of uncertainties; these include the number of emitted photons and the photon-emission time (time jitter).⁹ Quantum-tomography (QT) experiments are based on coincidence measurements, where one projects ρ_{ph} onto the two-photon subspace spanned by the basis

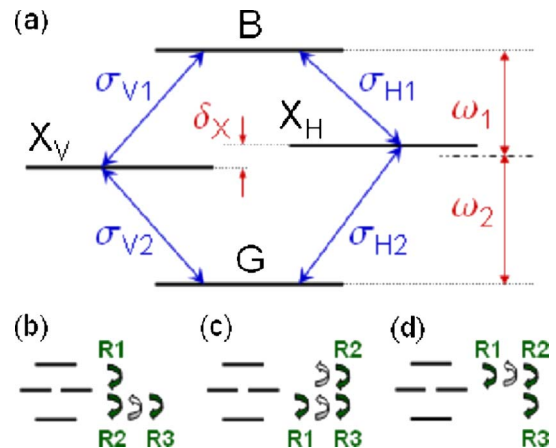


FIG. 1. (Color online) (a) Level scheme of the QD, including the ground state G , the linearly polarized excitons X_V and X_H , and the biexciton B . The optical transitions between them are induced by photons with linear polarization, frequencies $\omega_n \pm \delta_X/2$ ($n = 1, 2$), and represented by the ladder operators $\sigma_{H1} = |X_H\rangle\langle B|$, $\sigma_{H2} = |G\rangle\langle X_H|$, $\sigma_{V1} = |X_V\rangle\langle B|$, and $\sigma_{V2} = |G\rangle\langle X_V|$. (b)–(d) Examples of excitation (white) and relaxation [green (dark)] sequences, leading to the emission of more than two photons.

$\{|H1, H2\rangle, |H1, V2\rangle, |V1, H2\rangle, |V1, V2\rangle\}$.^{4,5} The corresponding two-photon density matrix is

$$\rho_{ph}^{QT} = \begin{pmatrix} \alpha_{HH} & \gamma_1 & \gamma_2 & \gamma \\ \gamma_1^* & \beta_{HV} & \gamma_3 & \gamma_4 \\ \gamma_2^* & \gamma_3^* & \beta_{VH} & \gamma_5 \\ \gamma^* & \gamma_4^* & \gamma_5^* & \alpha_{VV} \end{pmatrix}. \quad (1)$$

While the ideal state $|\psi\rangle$ corresponds to setting $\beta_{HV}=\beta_{VH}=0$, $\gamma_{1-5}=0$, and $|\gamma|=\alpha_{HH}=\alpha_{VV}=1/2$, the presence of imperfections and the same exciting conditions causes departures from ideality; these result specifically in $|\gamma|<\alpha$ and $\beta>0$ (see below for a discussion of the remaining terms). Here, we shall be concerned with both the degree of entanglement of ρ_{ph}^{QT} and its overlap with the overall radiation state ρ_{ph} . This determines the quality of a dot-based source of entangled photon pairs, beyond what is estimated by QT.

A. Dynamics of the dot-cavity system

The state of the emitted radiation can be derived from that of the QD-MC system (ρ). This is defined in the Hilbert space spanned by the states $\{|\chi, n_H, n_V\rangle\}$, where $\chi=G, X_H, X_V, B$ is the dot state, and (n_H, n_V) are the number of photons in the two degenerate cavity modes, with horizontal and vertical polarizations, respectively. The time evolution of ρ is computed by solving the following master equation, within the Born-Markov and rotating-wave approximations^{10,11} ($\hbar=1$):

$$\dot{\rho} = i[\rho, H] + (\mathcal{L}_{QD}^r + \mathcal{L}_{QD}^p + \mathcal{L}_{QD}^d + \mathcal{L}_{MC})\rho. \quad (2)$$

$H=H_{int}+H_{QD}+H_{MC}$, where

$$H_{int} = \sum_{\zeta=H,V} \sum_{i=1}^2 g_{\zeta i} (\sigma_{\zeta i}^{\dagger} a_{\zeta}^{\dagger} + \sigma_{\zeta i}^{\dagger} a_{\zeta}) \quad (3)$$

is the Jaynes-Cummings Hamiltonian that accounts for the dot-cavity interaction, where $\sigma_{\zeta 1} \equiv |X_{\zeta}\rangle\langle B|$, $\sigma_{\zeta 2} \equiv |G\rangle\langle X_{\zeta}|$, and a_{ζ} are the cavity-photon destruction operators. The noninteracting dot Hamiltonian reads

$$H_{QD} = (\omega_1 - \delta_X/2)|X_V\rangle\langle X_V| + (\omega_1 + \delta_X/2)|X_H\rangle\langle X_H| + (\omega_1 + \omega_2)|B\rangle\langle B|, \quad (4)$$

while the cavity contribution is $H_{MC}=\sum_{\zeta=H,V}\omega_{\zeta}a_{\zeta}^{\dagger}a_{\zeta}$.

The QD is coupled to a number of reservoirs that exchange energy with it and induce dephasing. In particular, the radiative relaxation induced by the photonic bath (leaky modes) is accounted for by the following Liouvillian:

$$\mathcal{L}_{QD}^r = \sum_{\zeta=H,V} \sum_{i=1,2} \frac{\Gamma_{\zeta i}^r}{2} \mathcal{L}(\sigma_{\zeta i}^{\dagger}) + \sum_{\{sec\}} \Gamma_{\zeta i, \xi j}^r \sigma_{\zeta i}^{\dagger} \rho \sigma_{\xi j}^{\dagger},$$

where $\mathcal{L}(A)\rho=2A\rho A^{\dagger}-A^{\dagger}A\rho-\rho A^{\dagger}A$ (Lindblad operators). Following the secular approximation, we have restricted the last summation to $(\zeta i, \xi j)=(H1, V2), (V1, H2)$. Throughout the paper, we consider the case of an incoherently pumped QD, where the laser generates electron-hole pairs in the continuum (wetting layer). These subsequently relax into the

dot. The corresponding Liouvillian \mathcal{L}_{QD}^p takes the form

$$\mathcal{L}_{QD}^p = \sum_{\zeta=H,V} \sum_{i=1,2} \frac{\Gamma_{\zeta i}^p}{2} \mathcal{L}(\sigma_{\zeta i}^{\dagger}) + \sum_{\{sec\}} \Gamma_{\zeta i, \xi j}^p \sigma_{\zeta i}^{\dagger} \rho \sigma_{\xi j}^{\dagger},$$

where the Γ are modulated by the laser intensity. In addition, virtual transitions involving phonons tend to induce (pure) dephasing:

$$\mathcal{L}_{QD}^d = - \sum_{\substack{\chi, \chi'=G, \\ X_H, X_V, B}} \frac{\gamma_{\chi\chi'}^d}{4} (|\chi\rangle\langle\chi|\rho|\chi'\rangle\langle\chi'| + |\chi'\rangle\langle\chi'|\rho|\chi\rangle\langle\chi|).$$

Finally, the coupling between the confined cavity modes and the external ones, and the resulting photon loss from the MC, are accounted for by $\mathcal{L}_{MC}=\sum_{\zeta=H,V}\kappa_{\zeta}\mathcal{L}(a_{\zeta})/2$. In the following, we assume the coupling constants, as well as the pumping and decoherence rates, not to depend on polarization. Consequently, $\alpha_{HH}=\alpha_{VV}\equiv\alpha$ and $\beta_{HV}=\beta_{VH}\equiv\beta$.

B. Correlation functions

The emission process produces radiation in a mixed state, from which the two-photon coincidence measurements single out ρ_{ph}^{QT} . Its matrix elements, experimentally reconstructed^{2,4-8} by means of the tomographic method,^{12,13} theoretically correspond to a specific set of (time-averaged) second-order correlation functions. In particular, if the photons at the frequencies ω_1 and ω_2 are emitted directly by the dot into the leaky modes, the diagonal terms in ρ_{ph}^{QT} are

$$\alpha = A \int_{t_m}^{t_M} \int_{t'_m}^{t'_M} dt dt' \langle \sigma_{H1}^{\dagger}(t) \sigma_{H2}^{\dagger}(t') \sigma_{H2}(t') \sigma_{H1}(t) \rangle,$$

$$\beta = A \int_{t_m}^{t_M} \int_{t'_m}^{t'_M} dt dt' \langle \sigma_{H1}^{\dagger}(t) \sigma_{V2}^{\dagger}(t') \sigma_{V2}(t') \sigma_{H1}(t) \rangle. \quad (5)$$

Here the normalization constant A is such that $2(\alpha+\beta)=1$, while t_m and t_M (t'_m and t'_M) define the temporal window related to the detection of frequency ω_1 (ω_2). The off-diagonal terms in ρ_{ph}^{QT} are instead

$$\langle \mu 1, \nu 2 | \rho_{ph}^{QT} | \xi 1, \zeta 2 \rangle = A \int_{t_m}^{t_M} \int_{t'_m}^{t'_M} dt dt' \times \langle \sigma_{\mu 1}^{\dagger}(t) \sigma_{\nu 2}^{\dagger}(t') \sigma_{\zeta 2}(t') \sigma_{\xi 1}(t) \rangle. \quad (6)$$

If the emission of the photons with frequency ω_2 is mediated by the cavity, the ladder operators $\sigma_{\zeta 2}$ in Eq. (5) are replaced by a_{ζ} ($\zeta=H, V$). All the above correlation functions are computed by applying the quantum regression theorem.^{14,15}

Hereafter, we shall focus on the coherence $\gamma = \langle H1, H2 | \rho_{ph}^{QT} | V1, V2 \rangle$. All the other nondiagonal terms appearing in Eq. (1) (γ_{1-5}) are identically zero (this will be implicitly understood hereafter when referring to ρ_{ph}^{QT}). The physical reason for this is that the Hamiltonian appearing in the first term of Eq. (2) only couples (and thus creates coherences between) dot-cavity states that share the same labels H and V of the excitations. Therefore, the only coherences with

nonzero expectation value are those spontaneously generated by the radiative relaxation of the system along the two paths $B \rightarrow X_H \rightarrow G$ and $B \rightarrow X_V \rightarrow G$. It should be noted that the density matrix estimated by means of QT generally includes nonvanishing values for the elements γ_i . Such discrepancy with respect to the expectation values might be related to statistical fluctuations, and is therefore expected to decrease for a sufficiently high number of events.¹³

C. Energy-polarization entanglement

A number of criteria have been proposed to establish whether or not a given ρ is separable. According to the Peres separability criterion,¹⁶ ρ_{ph}^{OT} is entangled if and only if $|\gamma| > \beta$. As far as a two-qubit system is concerned, the degree of entanglement is usually quantified by the concurrence¹² C . In the specific case we are considering, it is easily shown that $C=2(|\gamma|-\beta)$ for $|\gamma| > \beta$, and $C=0$ otherwise. Three main effects degrade the ideal (maximally entangled) ρ_{ph}^{OT} to a separable one: (i) the pure dephasing affecting the QD tends to quench the phase coherence of the intermediate state resulting from the first photon emission, $|X_H\rangle \otimes |H1\rangle + |X_V\rangle \otimes |V1\rangle$, and therefore to reduce $|\gamma|$; (ii) the energy splitting δ_X between the two excitonic states suppresses the interference terms by providing which-path information (reduced $|\gamma|$); (iii) the contribution to ρ_{ph}^{OT} of photons generated in different cascade emissions [see, e.g., Figs. 1(b)–1(d)] results both in a finite probability of observing counterpolarized 1 and 2 photons ($\beta > 0$) and in that of losing phase coherence between the H and V components of each photon type ($|\gamma| < \alpha$).¹⁷

III. RESULTS

A. Properties of the emitted radiation

For the sake of clarity, we start by considering the above effects separately, in the absence of a microcavity ($H_{int}=0$). The calculations reported in Fig. 2(a) isolate the contribution of the pure dephasing (i): to this end, we set $\delta_X=0$ and initialize the QD to the biexciton state ($|\psi(0)\rangle=|B\rangle$), while $\mathcal{L}_{QD}^p=0$. We plot $|\gamma|$ as a function of the dephasing rate γ_d , normalized to the emission rate Γ_r , having set for simplicity $\Gamma_{\zeta i}^r=\Gamma_{\zeta i, \zeta j}^r=\Gamma_r$. Due to these highly idealized exciting conditions (δ -like laser pulse), there is no probability of the QD being reexcited after emission, and therefore for ρ_{ph}^{OT} to suffer from the mixing of different cascades. As a consequence, $\beta=0$ and the Peres criterion is trivially satisfied by any $\gamma \neq 0$. The fact that the points describe a single curve (i.e., that C depends on γ_d and Γ_r only through their ratio) provides clear evidence of the interplay between dephasing and photon emission rate: in fact, a fast emission of photon 2 reduces the time during which dephasing degrades the intermediate state of the dot-cavity system.¹⁸ (ii) The effect of the energy splitting δ_X is shown in Fig. 2(b), where we plot $|\gamma|$ as a function of $|\delta_X|/\Gamma_r$, with $\gamma_d=0$. Once again, $|\gamma|=C/2$ depends on the two parameters only through their ratio. In fact, an increased Γ_r results in an enhanced homogeneous linewidth of the excitonic transitions, and therefore increases the overlap between the wave packets corresponding to photons $H2$ and

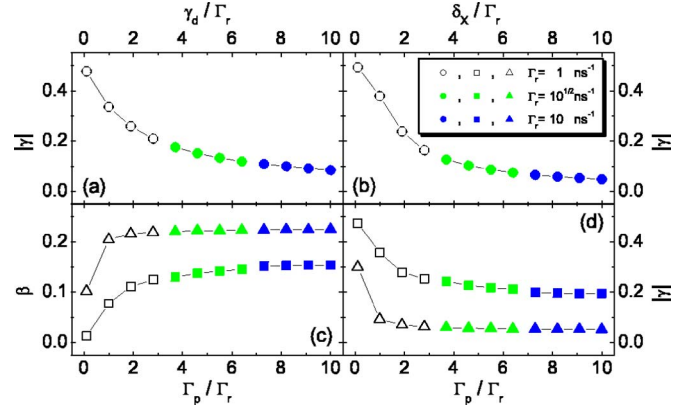


FIG. 2. (Color online) Values of β and $|\gamma|$ [see Eq. (1)] as a function of the dephasing rate γ_d (a), of the energy splitting δ_X (b), and of the pumping rate (c),(d). In the upper panels $\mathcal{L}_{QD}^p=0$ and the QD is initialized to the biexciton state, with $\delta_X=0$ (a) or $\gamma_d=0$ (b); in the lower panels, it is continuously pumped, with $|\psi(0)\rangle=|G\rangle$ and $\delta_X=\gamma_d=0$. In (a),(b) $t_m=t'_m=0$ and $t_M=t'_M=5/\Gamma_r$; in (c),(d) $t'_m=t_\infty$, $t'_M=t_\infty+1/\Gamma_r$ (squares) or $t'_M=t_\infty+5/\Gamma_r$ (triangles), $t_m=t_M=t_\infty$, t_∞ being large enough for the system to reach the stationary state.

V2.³ (iii) The possibility that ρ_{ph}^{OT} may include contributions from different cascades arises from the finite probability of reexciting the system between the first and the second photon emissions [Fig. 1(d)]. This explains the increment of β and the fall of γ with increasing excitation rate, for the case of a QD initialized in $|\psi(0)\rangle=|G\rangle$ and continuously pumped [Figs. 2(c) and 2(d), where $\gamma_d=\delta_X=0$]. In particular, we consider the case where a photon with frequency ω_1 is detected at some time t_∞ , after the stationary state has been achieved, and a finite temporal window ($\Delta t' \equiv t'_M - t'_m$) is available for the successive detection of a photon with frequency ω_2 . The value of $\Delta t'$ strongly affects that of β and γ . In fact, a shorter $\Delta t'$ reduces the probability, e.g., that the detected photons 1 and 2 might arise respectively from the relaxations R1 and R3 in Fig. 1(b). However, while this allows an increase of the measured concurrence of ρ_{ph}^{OT} , it does not improve the merits of the entangled-photon source, which depend on the state of the overall emission ρ_{ph} .

The above results allow us to isolate the contributions of different physical effects to the degradation of the ideal ρ_{ph}^{OT} , and thus provide upper limits on the value of C corresponding to each γ_d , Γ_p , or δ_X . The incidence of each of these factors was seen to strongly depend on the emission rate of photon 2. Therefore, in the following we shall analyze the case where such emission rate is increased by embedding the QD in a semiconductor MC close to resonance with the excitonic transition ($\omega_c=\omega_2$). In addition, we shall focus on the case of pulse-pumped excitation,^{4–6} which allows one to trigger the generation of photon pairs and to reduce the probability of unwanted reexcitations of the dot after the first cascade. In the weak-coupling regime, the effect of the QD-MC interaction essentially consists in enhancing the photon emission rate by a factor corresponding to the so-called Purcell factor $F_p=2g^2/\kappa\Gamma_r$. The parameters α , β , and γ corresponding to the cavity emission are computed by replacing in Eq. (5) the operators $\sigma_{\zeta 2}$ with a_ζ ($\zeta=H, V$).

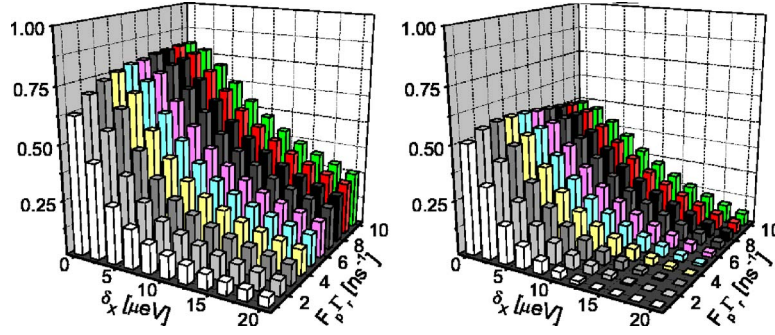


FIG. 3. (Color online) Concurrence of ρ_{ph}^{QT} as a function of the energy splitting δ_X and the cavity-assisted photon emission rate $F_p \Gamma_r$. Results are shown for the case of a short Gaussian pulse ($\sigma=10$ ps, $\Gamma_p=0.05$ ps $^{-1}$, left panel) and for a long one ($\sigma=100$ ps, $\Gamma_p=0.005$ ps $^{-1}$, right panel), with $t_m=t'_m=0$ and $t_M=t'_M=\infty$. Other physical parameters are $\Gamma_r^{-1}=10^3$ ps, $\gamma_d^{-1}=500$ ps, $g_{H2}=g_{V2}=0.05$ meV.

In Fig. 3 we plot the values of the concurrence as a function of the energy splitting δ_X and of the emission rate $F_p \Gamma_r$. No restriction is assumed with respect to the time delay between the detection of the two photons: $t_m=t'_m=0$, $t_M=t'_M=\infty$. For a relatively short exciting pulse (Gaussian time profile, with $\sigma=10$ ps) and δ_X not larger than a few μeV (left panel), values of C of about 0.8 are achieved. While the dependence of C on δ_X is monotonic, that on the Purcell factor is characterized by the presence of a maximum. In fact, if $F_p \Gamma_r$ is too high with respect to the exciting rate Γ_p , the system tends to emit a photon from an excitonic level before being excited to state B (see below). As already mentioned, the fact that the photons 1 and 2 might proceed from different cascades [e.g., from the decays $R2$ and $R1$, respectively, in Fig. 1(c)] weakens the overall degree of polarization correlation. This feature is even more dramatic in the case of a large and weaker exciting pulse (right panel, $\sigma=100$ ps), where it results in a strong suppression of the concurrence and in a displacement of the maximum toward lower values of F_p . Therefore, while increasing the Purcell factor allows one to suppress the detrimental effects of dephasing and of the exciton energy splitting δ_X (see Fig. 2), large values of F_p result in an overall reduction of the frequency-polarization entanglement.

B. Effects of the detection efficiency

A good source of entangled photon pairs is one where the probability p of emitting only two photons from a single cascade ($B \rightarrow X \rightarrow G$) is high as compared to those of the competing processes such as, for instance, those shown in Figs. 1(b)–1(d). In order to estimate such probabilities and to gain a deeper understanding of the underlying processes, it is useful to distinguish between the properties of the radiation emitted by the QD-MC system and those of the detected photons. To this aim we include the quantum feedback of the continuous measurement on the dot-cavity system.^{3,19,20} In particular, the evolution conditioned upon not having detected any photon up to time t is obtained by applying to the Liouvillians \mathcal{L}_{QD}^r and \mathcal{L}_{MC} the following substitutions:

$$\mathcal{L}_{MCP} \rightarrow \mathcal{L}_{MCP} - \eta_{MC} \sum_{\zeta=H,V} a_{\zeta} \rho a_{\zeta}^{\dagger},$$

$$\mathcal{L}_{QD}^r \rho \rightarrow \mathcal{L}_{QD}^r \rho - \eta_{QD} \sum_{\zeta=H,V} \sum_{n=1,2} \sigma_{\zeta n} \rho \sigma_{\zeta n}^{\dagger}, \quad (7)$$

where η_{QD} (η_{MC}) is the efficiency of the detectors times the collection efficiency of the photons emitted by the cavity (dot). The unconditioned dynamics considered so far therefore corresponds to the limit $\eta_{QD}, \eta_{MC} \ll 1$. The probability that the first detected photon has polarization ζ , and is generated by the relaxation of the dot into the leaky modes or by the cavity loss, is given, respectively, by

$$p_{\zeta n} = \Gamma_r \eta_{QD} \int_{t_m}^{t_M} dt \langle \sigma_{\zeta n}^{\dagger}(t) \sigma_{\zeta n}(t) \rangle, \\ p_{\zeta c} = \kappa \eta_{MC} \int_{t_m}^{t_M} dt \langle a_{\zeta}^{\dagger}(t) a_{\zeta}(t) \rangle, \quad (8)$$

where $\zeta=H, V$, $n=1, 2$. The joint probabilities that account also for the second photon detection take the form

$$p_{\zeta_1, \xi c} = B \int_{t_m}^{t_M} dt \int_t^{t_M} dt' \langle \sigma_{\zeta_1}^{\dagger}(t) a_{\xi}^{\dagger}(t') a_{\xi}(t') \sigma_{\zeta_1}(t) \rangle, \\ p_{\zeta_1, \xi_2} = B' \int_{t_m}^{t_M} dt \int_t^{t_M} dt' \langle \sigma_{\zeta_1}^{\dagger}(t) \sigma_{\xi_2}^{\dagger}(t') \sigma_{\xi_2}(t') \sigma_{\zeta_1}(t) \rangle,$$

where $B = \kappa \eta_{MC} \Gamma_r \eta_{QD}$, $B' = (\Gamma_r \eta_{QD})^2$, and $\xi=H, V$.

In order to investigate the intrinsic emission properties of the dot-cavity system, we consider the ideal case where all the emitted photons are detected ($\eta \equiv \eta_{QD} = \eta_{MC} = 1$). In Fig. 4 we show the dependence of $p_{\zeta c}$ and $p_{\zeta n}$ on the Purcell factor (that on δ_X , not shown here, is negligible), for a QD excited by a Gaussian pulse. The consecutive emission of two photons with frequency ω_1 is highly improbable: $p_{\zeta_1, \xi_1} \leq 0.0025$ (0.007) for an excitation pulse width $\sigma=10$ ps (100 ps). Therefore, the probability p of emitting only two photons from a single cascade ($B \rightarrow X \rightarrow G$) is well approximated by the probability of emitting from the biexciton state first (solid lines): $p \approx p_{H1} + p_{V1}$. For $F_p \Gamma_r \gtrsim \Gamma_p$, the dot tends to relax from an excitonic state before being excited to B [Fig. 1(c)]; correspondingly, $p_{\zeta c}$ increases (dotted lines) at the expense of p_{ζ_1} , and thus of p . The above process, which is mainly responsible for the decrease of C at high values of

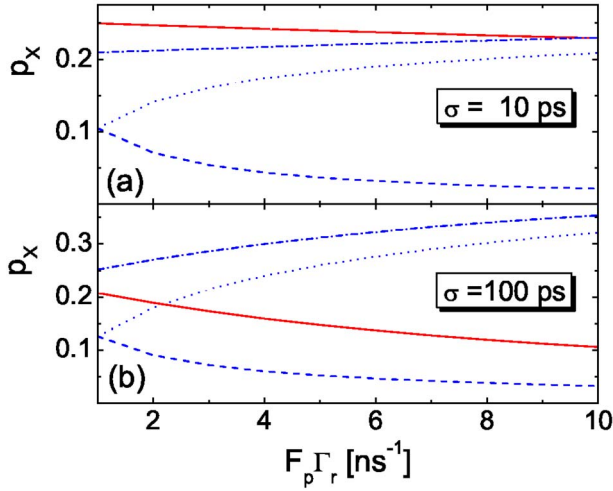


FIG. 4. (Color online) Probabilities associated with the first photon detection, as a function of $F_p \Gamma_r$ ($\delta_X=0$, $\eta_{QD}=\eta_{MC}=1$): $p_{\zeta 1}$ (solid lines), $p_{\zeta c}$ (dotted), $p_{\zeta 2}$ (dashed), $p_{\zeta c}+p_{\zeta 2}$ (dash-dotted), where $t_m=t'_m=0$, $t_M=t'_M=\infty$, and $\zeta=H, V$. In (a) $\sigma=10$ ps and $\Gamma_p=50$ ns $^{-1}$; in (b) $\sigma=100$ ps, $\Gamma_p=5$ ns $^{-1}$.

F_p (see Fig. 3), fixes an upper limit for the Purcell factor at each given excitation intensity. Such limitations, as well as those arising from the time jitter, might be possibly overcome by coherently exciting the QD with two-photon absorption processes.²¹

We finally note that the detection efficiency of the experimental apparatus can affect the degree of the entanglement estimated by means of QT for a given photon source. In fact, if the dot undergoes multiple cascades for each exciting pulse, the probability that the two detected photons arise from the same decay depends also on η . The representative

TABLE I. C and β as functions of $\eta_{MC}=\eta_{QD}\equiv\eta$ and of the pumping rate Γ_p , for $\sigma=100$ ps and $F_p=10$. The remaining physical parameters are the ones used in Fig. 3.

	C, β		
	$\eta=0.01$	$\eta=0.5$	$\eta=1$
$\Gamma_p=5$ ns $^{-1}$	0.200, 0.087	0.220, 0.080	0.250, 0.075
$\Gamma_p=10$ ns $^{-1}$	0.073, 0.120	0.110, 0.110	0.160, 0.098
$\Gamma_p=30$ ns $^{-1}$	0.000, 0.150	0.021, 0.120	0.110, 0.110

examples reported in Table I clearly show that, as η decreases, β increases and C is correspondingly reduced. This effect is most noticeable for higher exciting intensity, while it is suppressed in the limit of a single pair emission ($p \approx 1$).

IV. SUMMARY

The coupling of the QD with a MC and the resulting increase of the photon emission rate compensate the effect of dephasing and of the exciton energy splitting on the entanglement of emitted photon pairs. However, large Purcell factors result in an overall decrease of the polarization-frequency entanglement, for they increase the probability of multiple cascade decays. Finally, the effect of the Purcell factors on the measured concurrence is shown to grow with decreasing detection efficiency.

ACKNOWLEDGMENTS

This work has been partly supported by the Spanish MEC under Contracts No. MAT2005-01388 and No. NAN2004-09109-C04-4, by CAM under Contract No. S-0505/ESP-0200, and by the Italy-Spain “integrated action” No. HI2005-0027.

¹M. A. Nielsen and I. L. Chuang, *Quantum Computation and Quantum Information* (Cambridge University Press, Cambridge, U.K., 2000).

²O. Benson, C. Santori, M. Pelton, and Y. Yamamoto, *Phys. Rev. Lett.* **84**, 2513 (2000).

³T. M. Stace, G. J. Milburn, and C. H. W. Barnes, *Phys. Rev. B* **67**, 085317 (2003).

⁴N. Akopian, N. H. Lindner, E. Poem, Y. Berlatzky, J. Avron, D. Gershoni, B. D. Gerardot, and P. M. Petroff, *Phys. Rev. Lett.* **96**, 130501 (2006).

⁵R. M. Stevenson, R. J. Young, P. Atkinson, K. Cooper, D. A. Ritchie, and A. J. Shields, *Nature (London)* **439**, 179 (2006).

⁶R. J. Young, R. M. Stevenson, P. Atkinson, K. Cooper, D. A. Ritchie, and A. J. Shields, *New J. Phys.* **8**, 29 (2006).

⁷D. Fattal, K. Inoue, J. Vuckovic, C. Santori, G. S. Solomon, and Y. Yamamoto, *Phys. Rev. Lett.* **92**, 037903 (2004).

⁸M. Benyoucef, S. M. Ulrich, P. Michler, J. Wiersig, F. Jahnke, and A. Forchel, *New J. Phys.* **6**, 91 (2004).

⁹A. Kiraz, M. Atature, and A. Imamoglu, *Phys. Rev. A* **69**, 032305 (2004).

¹⁰J. I. Perea and C. Tejedor, *Phys. Rev. B* **72**, 035303 (2005).

¹¹F. Troiani, J. I. Perea, and C. Tejedor, *Phys. Rev. B* **73**, 035316

(2006).

¹²D. F. V. James, P. G. Kwiat, W. J. Munro, and A. G. White, *Phys. Rev. A* **64**, 052312 (2001).

¹³J. B. Altepeter, E. Jeffrey, and P. G. Kwiat, in *Advances in Atomic, Molecular, and Optical Physics*, Vol. 52, edited by P. R. Berman and C. C. Lin (Academic, New York, 2005).

¹⁴C. Cohen-Tannoudji, J. Dupont-Roc, and G. Grynberg, *Atom-photon Interactions* (Wiley-Interscience, New York, 1992).

¹⁵G. W. Gardiner and P. Zoller, in *Quantum Noise* (Springer-Verlag, Berlin, 2004).

¹⁶A. Peres, *Phys. Rev. Lett.* **77**, 1413 (1996).

¹⁷We neglect the effect of the exciton-spin relaxation. See, e. g., M. Paillard, X. Marie, P. Renucci, T. Anand, A. Jbeli, and J. M. Crerard, *Phys. Rev. Lett.* **86**, 1634 (2001).

¹⁸Further calculations where $\Gamma_{\zeta 1}^r \equiv \Gamma_r^1$ and $\Gamma_{\zeta 2}^r \equiv \Gamma_r^2$ were changed independently, confirm that γ depends specifically on the latter, i.e., on the exciton relaxation rate.

¹⁹H. M. Wiseman, *Phys. Rev. A* **49**, 2133 (1994).

²⁰H. Carmichael, in *Statistical Methods in Quantum Optics* (Springer-Verlag, Berlin, 1999).

²¹I. A. Akimov, J. T. Andrews, and F. Henneberger, *Phys. Rev. Lett.* **96**, 067401 (2006).